

Query Attack by Multi-Identity Surrogates

Sizhe Chen, Zehao Huang, Qinghua Tao, Xiaolin Huang, *Senior Member, IEEE*

Abstract—Deep Neural Networks (DNNs) are acknowledged as vulnerable to adversarial attacks, while the existing black-box attacks require extensive queries on the victim DNN to achieve high success rates. For query-efficiency, surrogate models of the victim are used to generate transferable Adversarial Examples (AEs) because of their *Gradient Similarity (GS)*, i.e., surrogates’ attack gradients are similar to the victim’s ones. However, it is generally neglected to exploit their similarity on outputs, namely the *Prediction Similarity (PS)*, to filter out inefficient queries by surrogates without querying the victim. To jointly utilize and also optimize surrogates’ GS and PS, we develop QueryNet, a unified attack framework that can significantly reduce queries. QueryNet creatively attacks by multi-identity surrogates, i.e., crafts several AEs for one sample by different surrogates, and also uses surrogates to decide on the most promising AE for the query. After that, the victim’s query feedback is accumulated to optimize not only surrogates’ parameters but also their architectures, enhancing both the GS and the PS. Although QueryNet has no access to pre-trained surrogates’ prior, it reduces queries by averagely about an order of magnitude compared to alternatives within an acceptable time, according to our comprehensive experiments: 11 victims (including two commercial models) on MNIST/CIFAR10/ImageNet, allowing only 8-bit image queries, and no access to the victim’s training data. The code is available at <https://github.com/Sizhe-Chen/QueryNet>.

Impact Statement—Deep Neural Networks (DNNs) have been validated as vulnerable, while they are much harder to attack in real-world black-box settings. Existing methods require hundreds of queries on the victim DNN to perform an effective attack. By proposing a new perspective that gradient and prediction similarity are fundamentally different, this paper fosters the query-based attackers via stealing the victim model using neural architecture search with a novel sample evaluation. Our unified attack framework, namely QueryNet, reduces the average query times to break a DNN by an order of magnitude from current baselines. Because practical DNNs are inevitably subject to intense queries, our work reveals the significant adversarial threat in DNN applications and advocates for attention to securing DNNs in deployment. Our view on DNN similarities may also inspire future work on attacks and defenses by surrogate models.

Index Terms—adversarial learning, artificial intelligence in security, neural networks

I. INTRODUCTION

This work was partially supported by National Natural Science Foundation of China (61977046), Shanghai Science and Technology Program (22511105600), and Shanghai Municipal Science and Technology Major Project (2021SHZDZX0102).

S. Chen, Z. Huang, and X. Huang are with the Department of Automation, and the Institute of Medical Robotics, Shanghai Jiao Tong University, and also with the MOE Key Laboratory of System Control and Information Processing, 800 Dongchuan Road, Shanghai, 200240, P.R. China. e-mails: sizhe.chen@berkeley.edu, {kinght_h, xiaolin-huang}@sjtu.edu.cn. Q. Tao is with ESAT-STADIUS, KU Leuven, Belgium. email: qinghua.tao@esat.kuleuven.be. Corresponding author: Xiaolin Huang.

Manuscript received November 21, 2022, revised February 21, 2023, accepted March 12, 2023.

AS Deep Neural Networks (DNNs) develop into the mainstream tools in pattern recognition for their high performance, their vulnerabilities become non-negligible [1]–[5]. A widely-known fact is that DNNs are sensitive to maliciously crafted imperceptible perturbations [6]–[9], and the resulted *Adversarial Examples (AEs)* could fool well-trained victim DNNs [10]–[15]. In real-world scenarios, the attackers generally have no access to the architecture, parameters, training data, and algorithmic details of the victim, and thus the so-called *black-box attacks* [16]–[18] are needed, which commonly depend on querying for victim’s outputs to iteratively modify the sample. Existing black-box query attacks already have very high success rates, so currently, the main efforts are devoted to reducing the number of queries [19]–[22], which is generally based on the similarity between the victim and the *surrogate* models at attackers’ hands. Due to the similarity, it is expected that white-box AEs on surrogates can *transfer* to hurt the victim as well [6], [23], [24].

Successful transfer attacks from the surrogates rely on the *Gradient Similarity (GS)* between surrogates and the victim [25]–[27], because an AE is produced by adding surrogate’s gradients to the original sample. For example, the attack on attention [28], [29], a method with high transferability, essentially relies on the similarity in the attention heap map, calculated based on gradients. However, GS is only one aspect and there is another critical but mostly neglected factor in attacks, which is the *Prediction Similarity (PS)*. Specifically, if the surrogates’ predictions are similar to the victim’s ones, they could filter out inefficient AEs, and thus prevent queries of less promising samples [30]. Notice that GS and PS are not naturally consistent, e.g., [31] obtains a surrogate with high GS by querying and training, and its AEs transfer to the victim well, but the surrogates’ accuracy is very low, indicating that the PS is not good. Generally speaking, existing methods have not taken the full use of the surrogates by jointly exploiting their GS and PS, resulting in unsatisfactory attack performance, e.g., over 500 average queries in attacking ImageNet [32] models under $\ell_2 = 5$.

In this paper, we propose QueryNet to take advantage of surrogates’ multiple identities so that their GS and PS are jointly exploited and improved. QueryNet is a unified framework for score-based query attacks, and its overall structure is illustrated in Fig. 1. From an original sample, QueryNet crafts several transferable *candidate* AEs by surrogates (transferable attackers) and also uses surrogates (transferability evaluators) to decide on the most promising AE for the query. By novel usage of surrogates with multiple identities, QueryNet generates effective queries from diverse candidates, reducing extensive query times. Furthermore, QueryNet also increases query-efficiency by creatively adopting neural architecture search (NAS) to optimize surrogates. Reasons herein are that QueryNet

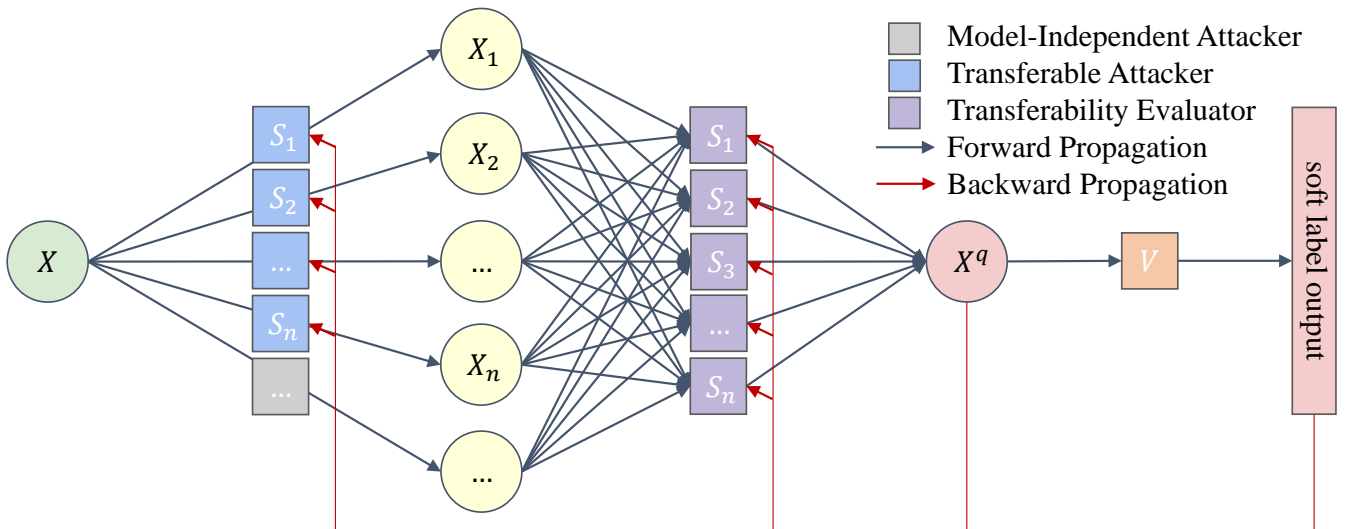


Fig. 1: QueryNet forward propagates to obtain query samples X^q towards the victim V (dark line), and the query pairs back propagate to optimize the surrogates (red line). In the forward propagation, we develop a novel manner to use multi-identity surrogates, i.e., not only as transferable attackers (blue) to craft candidate AEs X_i along with other attackers (grey), but also as transferability evaluators (purple) to decide on the most promising candidate AE X^q for the query. In the backward propagation, QueryNet creatively adopts NAS to train surrogates, increasing their GS and PS with X^q labeled by victim’s outputs. By the unified exploitation and improvement of both surrogate’s GS and PS, QueryNet reduces queries by about an order of magnitude.

does not take pre-trained surrogate’s knowledge, and attaining both high PS and GS in this case is challenging, requiring precise approximation to the victim from both the parameter and architecture aspect.

We comprehensively evaluate QueryNet with various state-of-the-art (SOTA) attacks proposed after 2019 under real-world settings: no access to the training data and only 8-bit image queries is allowed. Our experiments include 11 victims, two of which are commercial black-box models from the Baidu EasyDL platform [33]. Overall, QueryNet requires very few queries, reducing queries by 45% to 97% from the excellent SOTA Square attack [22] baseline. For example, when attacking WideResNet [34] under $\ell_2 = 3$, QueryNet reduces the average queries from 192.0 (baseline) to 5.3 on MNIST [35] and from 70.0 to 9.5 on CIFAR10 [36]. Besides, QueryNet uses only 24.0 average queries for definite fooling under $\ell_\infty = 0.05$ on MNASNet [37], an ImageNet [32] model. QueryNet achieves amazing query-efficiency within an acceptable amount of time due to our optimization and paralleling in implementation. Even with NAS, QueryNet only averagely consumes 0.15 to 0.65 seconds to craft an AE for MNIST and CIFAR10 victims under the common ℓ_∞ attack bounds.

We summarize our contributions as follows.

- We propose QueryNet, a unified attack framework, where surrogates’ GS and PS are jointly exploited in forward propagation and optimized in backward propagation.
- We design a novel AE evaluation mechanism in QueryNet’s forward propagation and creatively optimize surrogates by NAS in the backward propagation, forming an extremely query-efficient score-based attack.
- We comprehensively evaluate QueryNet under real-world settings, demonstrating that QueryNet reduces queries by averagely about an order of magnitude compared to recent

SOTA methods while maintaining the highest fooling rate.

The rest of this paper is organized as follows. In Section II, we will briefly introduce adversarial attacks, especially black-box query attacks and the surrogate models. The QueryNet is described in detail in Section III. Section IV evaluates QueryNet with baselines, presenting visual and numerical results to show QueryNet’s superiority. In Section V, a conclusion is given to end this paper with potential future work.

II. RELATED WORK

Adversarial attacks craft human-imperceptible perturbations on the input to mislead the victim DNN to make incorrect predictions. Since its proposal [38], many white-box attacks are developed [6]–[9], using the gradients of the victim to adversarially update the input, i.e., to increase the training loss, so that the victim produces false outputs with high confidence. White-box attacks generally achieve high success rates since the victim’s complete information is accessible, otherwise one has to adopt black-box attacks, which are generally categorized into transfer attacks [23], [24], [28], [39], [40] and query attacks [16]–[22]. Transfer attacks conduct white-box attacks on the surrogate model of the victim and expect the yielded AEs to hurt the victim, which is referred to as the attack transferability. The surrogate and the victim are both accurate, and thus are very similar in the prediction, but the attack transferability remains relatively low. In contrast, query attacks target a specific victim and update AEs iteratively according to the victim’s output feedback. They generally enjoy high success rates, but the number of queries leaves much to be reduced. According to the accessibility of the victim’s output, query attacks are further divided into score-based attacks [16]–[22] and decision-based ones [41]–[43]. The former ones provide the

probability vectors of the victim’s output for attackers, while the latter ones only allow access to the victim’s decisions, i.e., the top-1 predictions.

Score-based query attacks are our focus. Early studies try to estimate the victim’s gradients by additional queries around the sample [17], [44] inspired by white-box attacks, but this strategy is very query-intensive. Besides gradient estimation, fast pure random-search methods are also validated effective [21], [22], [45], which greedily update AEs only if the perturbation makes the sample more adversarial to the victim. Parallel methods introduce the surrogate model in transfer attacks to generate the transfer-prior, i.e., the initial adversarial perturbations [19], before querying the victim. Based on this idea, [25] regards surrogates’ transfer-prior as subspaces to reduce the query searching space; [26] adopts meta-learning to approximate the victim; [27] proposes to learn the victim’s (estimated) gradients via high-order computation graph. The aforementioned methods only exploit surrogates’ GS towards the victim to generate AEs. Recently, [30] uses surrogates’ PS for virtual queries on the victim, but it does not consider the GS and is resource-consuming due to the meta-training. Moreover, transfer attacks and random-search query attacks are still developing separately to the best of our knowledge.

Surrogates in query attacks can be trained differently. Most works train surrogates in a traditional way, i.e., decreasing the cross-entropy loss on the victim’s training data [19], [46] or external data [25]. Recently, [26], [30] propose to adopt meta-training to imitate the victim; [27] alters the loss to explicitly learn the victim’s (estimated) gradients; [31] trains a high-transferable AE generator from queries of no natural data; [47] models the conditional adversarial distribution by a conditional generative flow. The methods above consider the query data pair besides the victim’s training data. Comparatively, we only resort to query pairs. Also, we introduce NAS in training, because NAS optimizes the network in a larger space, i.e., modifying architectures besides parameters, which matches our need to precisely approximate the victim. Early NAS methods [48]–[50] consume much GPU resources. Differential ARchitecture Search (DARTS [51]) greatly reduces the cost of NAS by relaxing the search space to be continuous. Partially-Connected DARTS (PC-DARTS [52]) samples a small component of super-network to reduce the memory consumption without hurting the performance.

III. THE PROPOSED QUERYNET

In this section, we first introduce our notations and terminologies, then state our motivation to consider GS and PS by analyzing existing methods. After that, we present the design of QueryNet, especially the novel AE mechanism in the forward path and the creative NAS optimizing in the backward path. Finally, we summarize our QueryNet and the iterative query strategy in Alg. 1 and Alg. 2 respectively.

A. Preliminaries

The black-box attack problem is formulated as below. For an original \mathbf{x}^{org} that is correctly predicted by the victim as its

ground truth class y^{org} by a K -classifier victim V , the goal of the untargeted score-based query attack is to achieve

$$\begin{cases} \arg \max (\mathcal{V}(\mathbf{x}^{\text{adv}})) \neq y^{\text{org}}, \\ \|\mathbf{x}^{\text{adv}} - \mathbf{x}^{\text{org}}\|_p \leq \varepsilon, \\ \#\mathcal{V}(\mathbf{x}) \leq N, \end{cases} \quad (1)$$

where $\mathcal{V}(\mathbf{x}) : \mathbb{R}^d \mapsto \mathbb{R}^K$ represents the victim DNN with the prediction $[\mathcal{V}_1(\mathbf{x}), \dots, \mathcal{V}_K(\mathbf{x})]^T$.

The first condition in (1) means fooling the victim. In our QueryNet, we use the following margin loss

$$\mathcal{L}(\mathcal{V}(\mathbf{x}), y) = \mathcal{V}_y(\mathbf{x}) - \max_{k \neq y} \mathcal{V}_k(\mathbf{x}), \quad (2)$$

which stands for the smallest difference between victim’s output on the correct class and that on incorrect classes, and this is a simplified C&W attack loss [8]. If $\mathcal{L}(\mathcal{V}(\mathbf{x}), y^{\text{org}}) < 0$, the sample \mathbf{x} becomes an AE, and the attacker could also minimize surrogate’s margin loss to craft transferable examples. Since the query times for different samples vary a lot [53], the attack performance is generally evaluated on several images. Thus, in descriptions below, we uniformly denote a set of AEs as $X^{\text{adv}} = \{\mathbf{x}_k^{\text{adv}}\}$, and its counterpart original samples as X^{org} . Similarly, $\mathcal{V}(X)$ contains all predictions, and $L = \mathcal{L}(\mathcal{V}(X), Y)$ is the loss.

The second condition in (1) guarantees the attack imperceptibility, i.e., the perturbations are ℓ_p -norm bounded by ε , where p is commonly set as 2 or ∞ . The last condition in (1) is the budget for queries, meaning that the victim’s output $\mathcal{V}(\mathbf{x})$ is allowed to be accessed for no more than N times.

Besides our notations, we also summarize terminologies appeared in the introduction for a clear subsequent presentation.

- gradient similarity (GS): A surrogate has high GS if its gradients are similar to the victim, which is quantified by the attack transferability of its AEs towards the victim.
- transferable attacker: A surrogate is a transferable attacker if we use its gradients to generate AEs for the victim, i.e., exploiting its GS towards the victim.
- prediction similarity (PS): A surrogate has high PS if its predictions are similar to the victim, which is quantified by its prediction consistency with the victim.
- transferability evaluator: A surrogate is a transferability evaluator if we use it to evaluate and estimate the adversarial transferability of AEs, i.e., exploiting its PS towards the victim.
- multiple identities: refer to that surrogates are multiply exploited as transferable attackers and transferability evaluators in QueryNet.
- candidate AEs: crafted from the same original samples by different attackers, sent to the transferability evaluators as candidates for query samples.

B. Motivation

To attack in a query-efficient manner, surrogate models of the victim DNN have been adopted. The basic idea herein is to imitate the victim by the complete accessible surrogates at the attacker’s hands. The imitation is based on the similarity between the surrogate and the victim, which could be roughly divided into three levels.

TABLE I: Comparison with existing methods

Method	trainable components	attack by S (exploit GS)	predict by S (exploit PS)
Bandits [18]	×	×	×
NES [57]	×	×	×
RGF [58]	×	×	×
Transfer [23], [24]	×	single	×
P-RGF [19]	×	single	×
DaST [31]	S	single	×
Meta [26]	S	single	×
LeBA [27]	S	single	×
DPD [59]	distribution	single	×
CAD [47]	distribution	multiple	×
Subspace [25]	×	multiple	×
Simulator [30]	S	×	✓
QueryNet (ours)	S, \mathbf{w}	multiple	✓

Complete PS: The surrogate predicts exactly the same as the victim, leading to complete PS and GS. This unobtainable setting degrades black-box attacks to white-box ones.

High PS, Low GS: The surrogates’ outputs are quite similar to that of the victim, but their gradients differ distinctively. A direct example is the transfer attack, where surrogates share similar predictions with the victim due to the training on the same data, but surrogate’s AEs may not transfer to the victim since their GS is low. Although in this case, the attack transferability is not good, the high PS makes it promising to use the surrogate to decide whether an AE would hurt the victim or not [30]. This setting is achievable by training surrogates with victim’s training data or sufficient data labeled by the victim, which is similar to knowledge distillation [54] or model stealing attacks [55], [56].

Low PS, High GS: The attacker has little knowledge about the victim’s exact predictions, but could accurately guess its gradients, which could be realized without [17], [44] or with [19], [25] surrogates. Under this setting, white-box attacks on the surrogates are promising to craft transferable and efficient AEs towards the victim. But since the PS is low, the exact outputs of the victim cannot be well known and numerous queries are still needed.

According to the description above, we roughly categorize existing attacks in Table I. Commonly, the attack methods use one surrogate. More importantly, every surrogate only carries a single identity, i.e., is exploited either as an attacker due to their GS (column 3), or as a virtual predictor for their PS (column 4). Accordingly, the surrogate is utilized from a limited perspective, leading to great room for improving the attack performance. In this regard, it is imperative to develop a method that exploits multi-identity surrogates for both their GS and PS, and improves their GS and PS by accurate self-adjustments.

C. Craft queries by QueryNet: exploit GS and PS

In this paper, we propose a novel attack framework QueryNet. As illustrated in Fig. 1, QueryNet crafts the query samples by multi-identity surrogates in the forward propagation, and uses NAS to adjust surrogates by the victim’s feedback in the backward propagation.

Concretely, QueryNet first exploits surrogates’ GS and PS by generating various candidate AEs for one sample, and then selecting one of them with the highest (estimated) attack transferability X^q for the query, that is, the sample with the lowest surrogate’s margin loss. This novel usage of surrogates yields diverse AEs but only queries the victim with the most effective ones, reducing extensive query times. After that, QueryNet improves surrogates’ GS and PS by creatively adopting NAS to optimize the surrogates S , so that we could attack with better surrogates in the next query.

In the forward propagation, QueryNet first crafts diverse candidate AEs X_i by attacker \mathcal{A}_i as $X_i = \mathcal{A}_i^\varepsilon(X, \cdot)$. After that comes the most significant and distinctive part of QueryNet, the self-evaluation of potential candidate AEs. The idea is to estimate an AE’s transferability towards the victim by its transferability towards all surrogates, which is accessible and quantifiable as a weighted sum of surrogates’ loss values. Accordingly, the overall forward propagation to craft the k^{th} query sample at one iteration could be expressed as

$$X_k^q = X_{a_k, k} = \mathcal{A}_{a_k}^\varepsilon(X_k, \cdot),$$

$$a_k = \operatorname{argmin}_i \sum_{j=1}^n w_j \mathcal{L}(S_j(\mathcal{A}_i^\varepsilon(X_k, \cdot)), Y_k^{\text{org}}). \quad (3)$$

The first equation means that the query sample X_k^q is from attacker a_k , because, according to the second equation, it produces the AE with the lowest weighted surrogates’ loss, i.e., the highest transferability toward surrogates. Here i, j stand for the indexes of the attacker, evaluator respectively. w_j is the evaluation weight for surrogate S_j , and \mathbf{a} is a vector containing indexes of the samples.

In this way, QueryNet constructs a novel strategy to exploit not only surrogates’ GS to craft AEs but also their PS to filter out ineffective queries. Next, we discuss how we creatively improve GS and PS by query feedback to further reduce queries.

D. Self-adjustments in QueryNet: improve GS and PS

In the backward propagation, QueryNet adjusts its surrogates by the victim’s output. Instead of using pre-trained surrogates prior knowledge [19], [25], [27], our surrogates approximate V by training only on past query pairs $D = (X^q, \mathcal{V}(X^q))$ to minimize an MSE loss as in [26], [27], [30], i.e.,

$$\min_S \sum_{j=1}^n \|\mathcal{S}_j(\mathbf{x}) - \mathcal{V}(\mathbf{x})\|_2^2, \quad \mathbf{x} \in D. \quad (4)$$

Unlike existing methods [26], [27], QueryNet exploits multi-identity surrogates by using them as transferable attackers and transferability evaluators, pursuing high similarity on both prediction and gradient, which raises a higher requirement on surrogate’s approximation of the victim than focusing on one part. Therefore, in the self-adjustment of QueryNet, we alter also surrogates’ architectures by NAS. NAS optimizes DNN’s parameters and architecture by the training data and validation data respectively. The query pairs are generated naturally as the attack proceeds. For example, in attacking 9500 correctly-classified samples, we first add perturbations to them and query a victim. Then according to the query feedback,

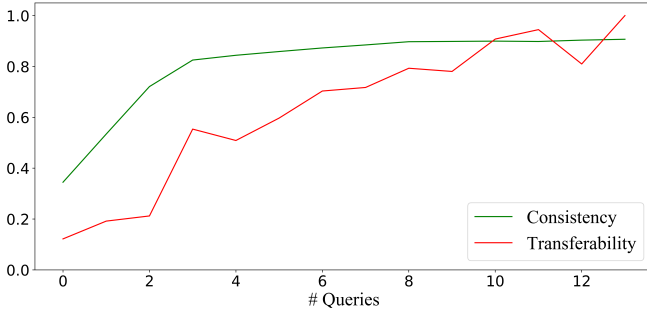


Fig. 2: The trend of surrogates’ consistency (PS), the attack transferability (GS) after every attack iteration (querying all 10K test samples). The consistency refers to the rate of similar predictions made by V and S on all past queries. The transferability is calculated by the victim’s error rates on the surrogate’s AEs from all original test samples, and we normalize them to make the largest value as 1 for a clear demonstration. The results are generated from attacking DenseNet40 [60] on MNIST with $\ell_2 = 3$.

500 adversarial examples are successfully crafted, so we repeat the same query process for the rest of 9000 samples, and get 9500+9000=18500 query pairs in total after 2 attack iterations. In the later iterations, more query pairs would be similarly generated and recorded for optimizing QueryNet surrogates’ parameters and architecture by randomly sampling from all query pairs. This step is denoted as $S' = \mathcal{O}(S, D)$, meaning that the surrogate is trained from S to S' until convergence. In this paper, PC-DARTS [52] is adopted here for its high performance and efficiency on time and memory.

Through our novel NAS training for attackers, the PS and GS of surrogates both increase during the attack, leading to a precise approximation for the victim. We demonstrate this by an example in Fig. 2. The PS (indicated by consistency) and GS (indicated by transferability) quickly increase after a few attack iterations, validating the effectiveness of our NAS optimization. The query time here means average query for each sample, and since attackers generally produce many AEs [27], [30], [59], the data is sufficient for convergence on a good solution.

Algorithm 1 QueryNet

Input: Pre-update samples X , labels Y , attack bound ε , victim V , surrogates S , past query pairs D , evaluation weights w , NAS method \mathcal{O} , attackers \mathcal{A} .

Output: query samples X^q

- 1: $X_i = \mathcal{A}_i^\varepsilon(X, \cdot)$ # craft candidate AEs with or without S
 - 2: $a_k = \operatorname{argmin}_i \sum_{j=1}^n w_j \mathcal{L}(S_j(\mathcal{A}_i^\varepsilon(X_k, \cdot)), Y_k^{\text{org}})$
 - 3: $X_k^q = X_{a_k, k}$ # select AEs with the highest transferability
 - 4: $D = D \cup (X^q, \mathcal{V}(X^q))$ # store the query feedback
 - 5: $S_i = \mathcal{O}(S_i, D)$ for $i = 1 \rightarrow n$ # NAS on S by (4)
 - 6: Update w according to (6) # estimate surrogates’ quality
 - 7: **return** X^q
-

Algorithm 2 Iterative Query Strategy for QueryNet

Input: Original samples X^{org} , labels Y^{org} , attack bound ε , maximum query N , victim V , number of surrogates n , evaluation weights w , NAS method \mathcal{O} , attackers \mathcal{A} .

Output: adversarial examples X^{adv}

- 1: $X^{\text{adv}} \leftarrow X^{\text{org}}, L^{\text{adv}} \leftarrow \mathcal{L}(\mathcal{V}(X^{\text{adv}}), Y^{\text{org}})$
 - 2: $D \leftarrow (X^{\text{adv}}, \mathcal{V}(X^{\text{adv}}))$ # store all past query pairs
 - 3: $S = [S_1, S_2, \dots, S_n] \leftarrow$ random initialization
 - 4: $S_i = \mathcal{O}(S_i, D)$ for $i = 1 \rightarrow n$ # train by initial queries
 - 5: **repeat**
 - 6: $F = \{k : L_k^{\text{adv}} > 0\}, (X, Y, L) = (X_F^{\text{adv}}, Y_F^{\text{org}}, L_F^{\text{adv}})$
 - 7: Get query samples X^q by QueryNet (Alg. 1)
 - 8: $I = \{k : L_k^q < L_k\}, (X_{F_I}^{\text{adv}}, L_{F_I}^{\text{adv}}) = (X_I^q, L_I^q)$
 - 9: **until** N times or X_F^{adv} is \emptyset
 - 10: **return** X^{adv}
-

E. QueryNet algorithm: a summary

The aforementioned QueryNet, including the forward propagation and backward propagation, is summarized in Alg. 1. In the forward propagation, we design a novel strategy to evaluate diverse candidate AEs, which are generated by various attackers. Among them, surrogate attackers are used for their GS to attack by FGSM [6]. Besides, two model-independent attacks are also involved to diversify the attack, which are the excellent Square attack [22] and Square+, a variant of Square attack designed by us. Details of all attackers are presented in Appendix A. In the backward propagation, we creatively adopt NAS to optimize surrogates by the query pairs. In this way, surrogates’ GS and PS increase quickly during the attack as in Fig. 2. Besides improving the quality of a surrogate, we also pay attention to calibrating its quality. Thus, we also learn surrogates’ evaluation weights w by the victim’s feedback, which is specified in Appendix B.

Before we have discussed how to attack in one iteration by QueryNet, next we present the iterative query attack strategy for QueryNet in Alg. 2. The procedure starts by training randomly initialized surrogates with query pairs of original samples $(X^{\text{org}}, \mathcal{V}(X^{\text{org}}))$. At each attack iteration, we only focus on unsuccessful AEs X , i.e., those correctly predicted by V (line 6 in Alg. 2). Then we use QueryNet to craft X^q to query the victim. Finally, we update our AEs by those that become more adversarial to the victim (line 8 in Alg. 2), i.e., always hold the “most adversarial” examples with the smallest victim’s loss.

By the iterative implementation, QueryNet’s novel AE evaluation mechanism and creative NAS training dramatically increase the query-efficiency by exploiting and improving multi-identity surrogates’ GS and PS in a unified framework, which is validated by our extensive experiments below.

IV. EXPERIMENTS

A. Setup

Baselines. We evaluate QueryNet along with several SOTA attacks proposed after 2019, which are Bandits [18], Subspace [25], LeBA [27], PPBA [45], SimBA [21], and Square [22]. Notice that most of the attacks are originally tested on CIFAR10 and we select the most efficient ones, including Bandits, PPBA,

TABLE II: Dataset and the attack bound ε

Dataset	Image Size	Data	Test Data	$\varepsilon (l_\infty)$	$\varepsilon (l_2)$
MNIST	$28 \times 28 \times 1$	70K	10K	0.3	3
CIFAR10	$32 \times 32 \times 3$	60K	10K	16 / 255	3
ImageNet	$224 \times 224 \times 3$	1300K	1K	0.05	5

Subspace, and Square for MNIST and ImageNet. For the compared methods, we generally inherit the default hyper-parameters from their papers, seeing Appendix C. Results show that QueryNet, using only randomly-initialized surrogates, outperforms all baselines, even those using pre-trained surrogates’ prior knowledge [25], [27].

Metrics. In all empirical studies, we conduct untargeted attack until iteration $N = 10000$, i.e., the maximum query times, and report the victim’s remaining accuracy on all samples (Acc.), the average query times (A.Q.), and the median query times (M.Q.) for only successful AEs, which is also the setting in [16], [21], [22]. A.Q., rather than the total queries, is the main concern for query-based attacks. The reason herein is that A.Q. directly signifies the concealment of attacks. High A.Q. means many queries with similar AEs from the same original sample, which are highly detectable by defenders. By contrast, low A.Q. means queries with samples of mostly different objects, which behave like normal usage of DNNs. Thus, it is reasonable for [27], [30], [59] and us to reduce A.Q. by using different query samples to train surrogates. And the data for NAS training is sufficient, e.g., 2 A.Q. for 10K test images in MNIST yields 20K training data for surrogates.

Victims. We attack various victims including WideResNet10 (WRN10 [34]), ResNet with Pre-activation (RNP [61]), and DenseNet40 (DN40 [60]) for MNIST, WideResNet28 (WRN28 [34]), GDAS [62], and PyramidNet272 (PyrN272 [63]) for CIFAR10, InceptionV3 (IncV3 [64]), ResNetX101 (RNx101 [65]), and MNASNet (MNASNet [37]) for ImageNet. Victims are pre-trained models from Torchvision [66] for ImageNet, official repositories for CIFAR10, and our training for MNIST from [67]. To evaluate QueryNet on real-world black-box settings, we also attack 2 commercial APIs from Baidu EasyDL [33], where we have no knowledge about the victims but could only get its output probability. We use PyTorch [66] platform with 4 NVIDIA Tesla V100 GPUs, and the report of QueryNet’s time consumption is based on these devices.

Dataset. Information about the dataset and the attack bound is specified in Table II, where columns 3 and 4 show the sample number in the dataset and our evaluation, respectively. For ImageNet, we randomly select one image from each of the 1K categories in the validation set and resize the samples into 224 resolution for the victim’s and surrogates’ inputs. We use all 10K samples in the MNIST/CIFAR10 test set. To the best of our knowledge, no such large-scale experiment has been conducted for query-based attacks. For attack bounds, we mostly adopt common values (columns 5 and 6 in Table II).

Bit-depth. Existing methods, especially those requiring accurate gradient estimation, generally feed models with 32-bit images [22], [25], [27], [30]. However, real-world models generally accept only 8-bit image inputs. This makes a great

TABLE III: Influence of the 8-bit setting: study on ImageNet by ResNet50 (clean accuracy 87.91%)

		Acc.	A.Q.	M.Q.	Acc.	A.Q.	M.Q.
l_∞	RN50	32-bit query			8-bit query		
$\frac{16}{255}$	SimBA	10.2%	179.3	56	29.0%	486.7	81
	SimBA+	10.1%	178.4	54	26.7%	382.5	65
	SimBA++	4.0%	140.6	40	29.0%	405.3	56
	LeBA	1.1%	120.6	27	11.9%	538.8	45
$\frac{32}{255}$	SimBA	9.5%	212.7	32	11.9%	208.0	36
	SimBA+	6.7%	117.6	25	9.6%	158.3	34
	SimBA++	0.6%	42.3	5	5.1%	124.2	23
	LeBA	0.1%	33.2	3	0.6%	84.2	8

difference in performance evaluation, seeing our reproduction of [27] using 8-bit and 32-bit queries. According to Table III, restricting to 8-bit query input dramatically decreases the performance by a large margin. Thus, it is meaningful and significant for us to conduct large-scale evaluations in this real-world setting. We implement 8-bit setting by cutting the 32-bit query samples to 8-bit in the $[0, 255]$ image space, since all samples are rescaled to $[0, 1]$ and normalized according to the mean and the variance of the dataset in pre-processing.

NAS. In PC-DARTS, we inherit most hyper-parameters in [52], but change the number of layers for the diversity of surrogates. Concretely, we choose # layers as 6, 8, 10 for three surrogates on CIFAR10, and 3, 4, 5 for smaller surrogates on MNIST. We train by all past query pairs as randomly sampled mini-batches until convergence, i.e., the training MSE loss is lower than 2 after 30 iterations. If the loss does not decrease quickly enough, we also stop the training after 100 batches for time-efficiency, and we alter 100 to 1500 in the first iteration when surrogates should be thoroughly trained from scratch. The batch size is 300 for MNIST and 128 for CIFAR10.

B. Results

The attack performance is reported in Table IV, where “*” indicates the method uses surrogates pre-trained on the victim’s training set. Overall, QueryNet achieves a significant reduction in queries from the SOTA attacks, while maintaining the highest success rates. On MNIST, the A.Q. decreases from 192.0 to an amazing 5.3 in attacking WRN10, surpassing baselines by an order of magnitude. QueryNet reduces the victim’s accuracy from over 99.4% to below 0.7% in all conducted evaluations. And QueryNet also greatly surpasses BayesOpt [68] based on our assessment. Note that the attack performance is not good when A.Q. is small with a high Acc., e.g., PPBA in MNIST, because A.Q. and M.Q. neglects failed AEs.

On CIFAR10, a similar trend can be observed. QueryNet cuts down about 50% to 70% queries in l_∞ attacks and 75% to 85% queries in l_2 attacks from Square attack, which is already verified excellent. In all evaluations, QueryNet achieves a definite fooling within 30 A.Q. for a sample. The reduction of queries by QueryNet is significant in l_2 attacks, indicating that DNNs are vulnerable to l_∞ -unrestricted AEs. We also visualize our searched architecture in Appendix E.

QueryNet’s impact on decreasing A.Q. on ImageNet is also obvious, especially in l_2 attacks. It also decreases the M.Q.,

TABLE IV: The attack performance on MNIST, CIFAR10, and ImageNet

		Acc.	A.Q.	M.Q.	Acc.	A.Q.	M.Q.	Acc.	A.Q.	M.Q.
MNIST		WRN10 (99.41%)			RNP (99.59%)			DN40 (99.46%)		
ℓ_∞	Bandits	9.7%	149.7	26	13.9%	56.8	22	17.7%	62.9	16
	PPBA	7.7%	49.6	2	3.0%	205.8	2	8.4%	25.4	2
	Square	5.1%	50.2	28	1.1%	13.9	1	0.8%	46.2	22
	QueryNet	0.1%	3.9	2	0.7%	7.6	1	0.0%	5.0	4
ℓ_2	Bandits	29.7%	963.3	28	40.2%	1894.7	39	26.4%	175.8	18
	PPBA	7.0%	41.4	2	9.3%	14.6	2	8.9%	4.2	2
	Square	3.8%	192.0	58	3.2%	411.7	90	0.5%	184.3	53
	QueryNet	0.5%	5.3	4	0.4%	18.6	5	0.2%	5.9	4
CIFAR10		WRN28 (95.97%)			GDAS (97.19%)			PyrN272 (98.44%)		
ℓ_∞	Bandits	27.0%	785.8	66	38.2%	1177.1	127	54.0%	1166.6	145
	SimBA	13.3%	188.2	1	1.2%	50.5	1	32.9%	401.3	20
	LeBA*	5.1%	164.2	2	0.7%	24.0	1	18.8%	304.6	2
	PPBA	1.4%	78.6	2	1.1%	98.1	2	3.6%	202.1	2
	Subspace*	0.0%	65.0	24	0.0%	53.0	24	0.2%	136.6	34
	Square	0.0%	53.1	13	0.0%	15.6	1	0.0%	56.4	4
	QueryNet	0.0%	16.0	2	0.0%	5.0	1	0.0%	28.3	2
ℓ_2	Bandits	22.2%	329.9	20	18.5%	952.8	24	22.3%	1836.3	552
	SimBA	1.2%	81.4	7	0.2%	12.9	1	7.0%	282.9	27
	LeBA*	0.8%	57.1	2	0.2%	8.5	1	6.0%	235.9	2
	PPBA	0.2%	36.2	2	0.5%	84.4	2	0.4%	132.2	2
	Subspace*	0.1%	524.9	418	0.0%	474.7	440	0.0%	583.9	540
	Square	0.0%	70.0	22	0.0%	40.4	16	0.0%	106.2	63
	QueryNet	0.0%	9.5	2	0.0%	5.8	2	0.0%	24.3	3
ImageNet		IncV3 (77.45%)			RNX101 (79.31%)			MNASN (73.51%)		
ℓ_∞	PPBA	11.8%	627.9	42	7.8%	489.1	26	2.5%	284.9	10
	Subspace*	0.3%	114.1	22	0.0%	127.1	26	0.0%	37.5	16
	Square	0.2%	132.1	11	0.0%	82.3	15	0.0%	26.8	2
	QueryNet	0.3%	123.0	12	0.0%	79.8	12	0.0%	24.0	2
	QueryNet*	0.2%	74.7	3	0.0%	47.3	2	0.0%	13.5	2
ℓ_2	PPBA	19.8%	1333.9	540	4.6%	939.2	390	2.3%	683.9	291
	Subspace*	3.7%	1395.0	992	1.0%	1717.5	1289	0.2%	1250.5	971
	Square	3.6%	528.7	120	0.4%	630.6	160	0.1%	442.8	129
	QueryNet	2.8%	518.6	72	0.5%	481.8	96	0.0%	280.1	50
	QueryNet*	1.9%	263.5	4	0.2%	196.0	4	0.1%	125.1	3
EasyDL		MNIST (98.35%)			CIFAR10 (96.18%)					
ℓ_∞	Square	0.0%	3.4	1	0.0%	23.7	5			
	QueryNet	0.0%	2.4	1	0.0%	16.0	2			
ℓ_2	Square	0.0%	31.6	19	0.0%	28.1	9			
	QueryNet	0.0%	21.5	7	0.0%	14.4	2			

TABLE V: Ablation study on different attack bounds (CIFAR10, WRN28)

		Square Baseline			Ours \ (NAS & Square+)			Ours \ (NAS)			Ours (QueryNet)		
ϵ		Acc.	A.Q.	M.Q.	Acc.	A.Q.	M.Q.	Acc.	A.Q.	M.Q.	Acc.	A.Q.	M.Q.
ℓ_∞	4 / 255	4.3%	1372	675	3.8%	1300	612	3.7%	1292	595	3.2%	1103	380
	8 / 255	0.2%	365.6	119	0.1%	336.0	89	0.1%	323.5	89	0.1%	210.0	30
	12 / 255	0.0%	129.4	37	0.0%	102.9	20	0.0%	100.0	19	0.0%	47.6	3
	16 / 255	0.0%	53.1	13	0.0%	35.3	3	0.0%	33.6	3	0.0%	16.0	2
	20 / 255	0.0%	27.1	4	0.0%	15.5	2	0.0%	15.6	2	0.0%	6.7	2
ℓ_2	1	3.1%	807.5	256	3.1%	778.6	240	3.3%	762.0	245	2.4%	554.2	96
	2	0.2%	194.6	53	0.1%	168.2	41	0.1%	155.8	38	0.0%	26.8	4
	3	0.0%	70.0	22	0.0%	44.0	6	0.0%	42.7	7	0.0%	9.5	2
	4	0.0%	34.0	10	0.0%	16.7	3	0.0%	14.0	3	0.0%	5.0	2
	5	0.0%	17.5	4	0.0%	8.5	2	0.0%	7.0	2	0.0%	3.5	2

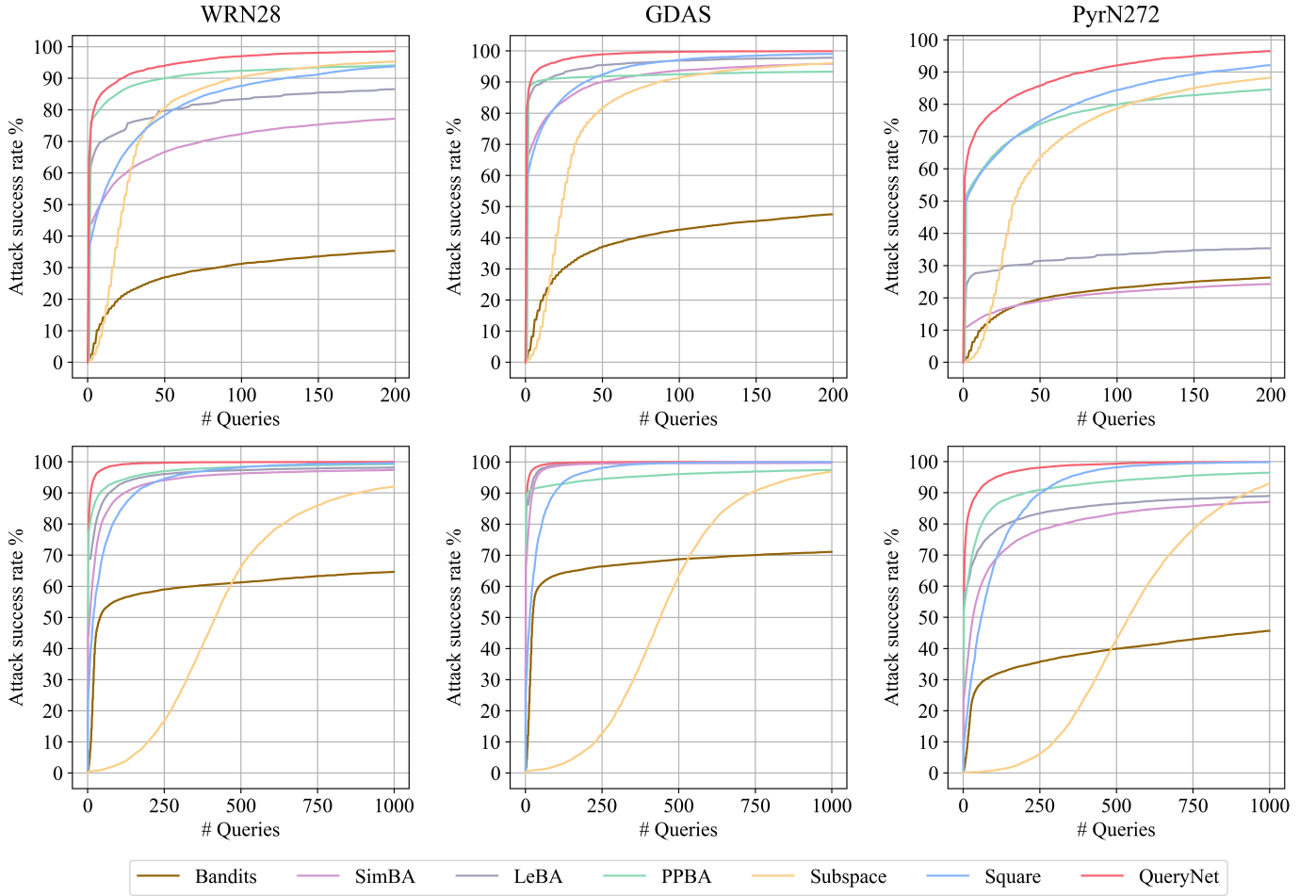


Fig. 3: The trend of attack success rates for different methods on CIFAR10 in Table IV. Top figures are for ℓ_∞ attacks and bottom ones are for ℓ_2 attacks.

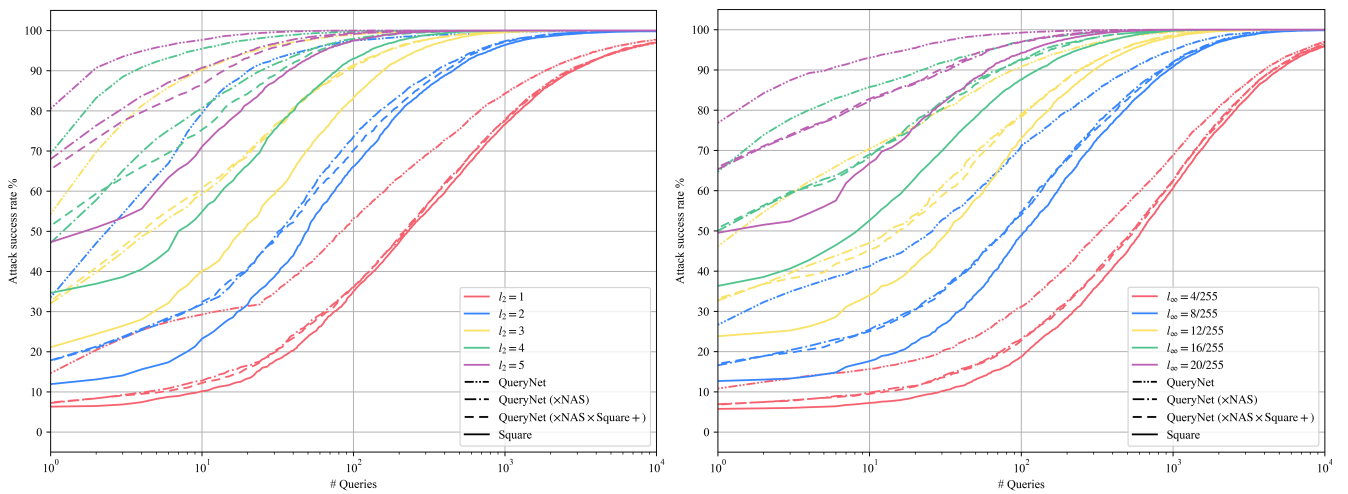


Fig. 4: The trend of attack success rates for Table V, in logarithmic axis.

reducing the victim’s accuracy very fast in initial iterations. Due to the computational consumption of NAS on ImageNet, we train the surrogates only once and do not finetune them later, thus only revealing QueryNet’s partial potential here. Still, QueryNet outperforms all baselines, especially in ℓ_2 attacks. For further reference, we also report results with pre-trained surrogates (DN121 [60], DN169 [60], and RN50 [69]) as QueryNet*, but that is not our main focus.

Baidu EasyDL [33] provides a platform for black-box attack evaluation, which is fair and more convincing, since no one can access the neural networks’ knowledge. For those models in Baidu EasyDL, both Square and QueryNet achieve definite fooling quickly, but the required number of queries in QueryNet is significantly smaller. Our experiments demonstrate that QueryNet remains very query-efficient in complete black-box settings, where we have no idea how the victims are built and trained. This experiment sounds alarmed that the existing commercial models on the platform are not robust and can be attacked within only a few queries, so that the defender [70]–[73] is hard to detect attacks based on the query times.

For a deeper illustration, we present the attack success rates after every query iteration in Fig. 3. In all performed experiments, QueryNet achieves high success rates very quickly in initial queries, resulting in low M.Q., and also efficiently modifies the remaining robust samples for the victim, leading to low A.Q. and Acc. The striking performance is obtained by our novel design to focus on surrogates’ PS and GS.

C. Ablation study

To investigate the influence of our major designs, we here conduct the ablation studies under different attack bounds. First, we exclude Square+ and NAS from QueryNet and report the performance using trainable surrogates (DenseNet121, DenseNet169, and ResNet50) in column 3 of Table V. One could observe that our strategy of surrogates’ multiple identities, ensemble, and learnable self-evaluation, and adjustable surrogates, could significantly reduce queries from Square attack baseline. Second, we additionally equip the Square+ attacker, and the attack performance is further improved (column 4). Finally, the complete QueryNet (column 5) obtains dramatic improvement, showing that NAS could lead to much better GS/PS and thus greatly contribute to the quality of surrogates. The success rate is plotted in Fig. 4. Every four lines with the same color also show that our novel designs all positively contribute to the final amazing performance.

To investigate the influence of the number of surrogates n , we construct different numbers of diverse surrogates by altering the number of layers in PC-DARTS, and perform each evaluation 5 times to reduce interference from randomness. The results are reported in Table VI. A natural conclusion here is that more surrogates lead to better and more stable attacks, but require more computation. For a trade-off, we select $n = 3$ in all remaining experiments in this paper. Notice that in the previous experiments, only one trial is tested.

D. Computation analysis

For adversarial attacks, the computation time is not very strict [74]. The proposed QueryNet indeed needs computation

TABLE VI: The attack performance and GPU hours with different n values (CIFAR10, WRN28, $\ell_\infty = \frac{16}{255}$, $\ell_2 = 3$)

	n	# Layers	Acc.	A.Q.	M.Q.	GPU
ℓ_∞	1	10	0.0%	16.85 ± 0.59	2	0.8
	3	6,8,10	0.0%	14.61 ± 0.29	2	2.3
	5	4,6,...,12	0.0%	13.29 ± 0.13	2	8.9
ℓ_2	1	10	0.0%	12.65 ± 0.29	3	1.1
	3	6,8,10	0.0%	8.76 ± 0.25	2	3.7
	5	4,6,...,12	0.0%	7.56 ± 0.22	2	15.7

TABLE VII: The time consumption of QueryNet, measured by total GPU hours and GPU seconds per image

	Victim	Acc.	A.Q.	M.Q.	GPU	per image
MNIST $\ell_\infty = 0.3$	WRN10	0.1%	3.9	2	6.1 hrs	2.20 s
	RNP	0.7%	7.6	1	2.4 hrs	0.86 s
	DN40	0.0%	5.0	4	1.6 hrs	0.58 s
CIFAR10 $\ell_\infty = \frac{8}{255}$	WRN28	0.1%	210	30	3.9 hrs	1.40 s
	GDAS	0.0%	62	6	4.3 hrs	1.55 s
	PyrN272	0.0%	219	70	7.2 hrs	2.59 s

to perform NAS. But QueryNet can be well implemented using parallel computing on data and model with early-stopping, then the overall time consumption is still acceptable. As in Table VII, QueryNet crafts one AE under common bounds within only 0.5 to 2.6 GPU seconds, i.e., 0.15s to 0.65s using 4 GPUs on average. In comparison, the recent Simulator attack [30] requires over 72 GPU hours to train the meta attacker before the first query. Also, ZOO [17] consumes an average of 56.35 seconds to successfully attack one CIFAR-10 image on WRN28, while QueryNet only needs 1.40 seconds. And Bandits, Subspace, LeBA, PPBA, and SimBA all conduct no data paralleling and is thus much slower than QueryNet. Therefore, QueryNet has no significant disadvantage on computation time.

V. CONCLUSION AND FUTURE WORK

We develop the QueryNet to exploit and improve both the GS and PS of surrogates to achieve great attack performance. The query-efficient comes from the novel usage of multi-identity surrogates as transferable attackers for their GS and transferability evaluators due to the PS. In our unified framework, surrogates are also creatively trained by NAS, further improving the performance. QueryNet reduces queries by about an order of magnitude while maintaining the highest fooling rate in our comprehensive and realistic evaluations.

Note that QueryNet cannot be applied to decision-based attacks by training surrogates with hard labels, because in this case, QueryNet still needs the model’s soft outputs to greedily decide whether a query sample is more adversarial. And in the future, it would be interesting to explore the surrogate’s usage in decision-based attacks. Also, it is possible to design other attackers on QueryNet, e.g., by adopting more extensible architecture space, more transferable white-box attacks, and more advanced NAS strategies. However, our attack is only applicable in digital space and thus does not exert imminent impacts to the deployed DNNs on life-concerning systems like physical attacks, which demand a stable invasion across cameras and sensors.

REFERENCES

- [1] A. Mustafa, S. H. Khan, M. Hayat, J. Shen, and L. Shao, "Image super-resolution as a defense against adversarial attacks," *IEEE Transactions on Image Processing (TIP)*, vol. 29, pp. 1711–1724, 2020.
- [2] H. Li, Y. Zeng, G. Li, L. Lin, and Y. Yu, "Online alternate generator against adversarial attacks," *IEEE Transactions on Image Processing (TIP)*, vol. 29, pp. 9305–9315, 2020.
- [3] Y. Xu, B. Du, and L. Zhang, "Self-attention context network: Addressing the threat of adversarial attacks for hyperspectral image classification," *IEEE Transactions on Image Processing (TIP)*, vol. 30, pp. 8671–8685, 2021.
- [4] Z. Zhao, H. Wang, H. Sun, J. Yuan, Z. Huang, and Z. He, "Removing adversarial noise via low-rank completion of high-sensitivity points," *IEEE Transactions on Image Processing (TIP)*, vol. 30, pp. 6485–6497, 2021.
- [5] S. Zhang, H. Gao, and Q. Rao, "Defense against adversarial attacks by reconstructing images," *IEEE Transactions on Image Processing (TIP)*, vol. 30, pp. 6117–6129, 2021.
- [6] I. J. Goodfellow, J. Shlens, and C. Szegedy, "Explaining and harnessing adversarial examples," in *International Conference on Learning Representations (ICLR)*, 2015.
- [7] S.-M. Moosavi-Dezfooli, A. Fawzi, and P. Frossard, "Deepfool: A simple and accurate method to fool deep neural networks," in *the IEEE/CVF Conference on Computer Vision and Pattern Recognition (CVPR)*, 2016, pp. 2574–2582.
- [8] N. Carlini and D. Wagner, "Towards evaluating the robustness of neural networks," in *the IEEE Symposium on Security and Privacy (SP)*, 2017, pp. 39–57.
- [9] A. Madry, A. Makelov, L. Schmidt, D. Tsipras, and A. Vladu, "Towards deep learning models resistant to adversarial attacks," in *International Conference on Learning Representations (ICLR)*, 2018.
- [10] S. Tang, X. Huang, M. Chen, C. Sun, and J. Yang, "Adversarial attack type I: Cheat classifiers by significant changes," in *IEEE Transactions on Pattern Analysis and Machine Intelligence (TPAMI)*, 2021, pp. 1100–1109.
- [11] Y. Zhang, X. Tian, Y. Li, X. Wang, and D. Tao, "Principal component adversarial example," *IEEE Transactions on Image Processing (TIP)*, vol. 29, pp. 4804–4815, 2020.
- [12] J. Wang, A. Liu, X. Bai, and X. Liu, "Universal adversarial patch attack for automatic checkout using perceptual and attentional bias," *IEEE Transactions on Image Processing (TIP)*, pp. 1–1, 2021.
- [13] Z. Che, A. Borji, G. Zhai, S. Ling, J. Li, Y. Tian, G. Guo, and P. Le Callet, "Adversarial attack against deep saliency models powered by non-redundant priors," *IEEE Transactions on Image Processing (TIP)*, vol. 30, pp. 1973–1988, 2021.
- [14] N. Li and Z. Chen, "Toward visual distortion in black-box attacks," *IEEE Transactions on Image Processing (TIP)*, vol. 30, pp. 6156–6167, 2021.
- [15] L. Wang and K.-J. Yoon, "Psat-gan: Efficient adversarial attacks against holistic scene understanding," *IEEE Transactions on Image Processing (TIP)*, vol. 30, pp. 7541–7553, 2021.
- [16] N. Papernot, P. McDaniel, I. Goodfellow, S. Jha, Z. B. Celik, and A. Swami, "Practical black-box attacks against machine learning," in *the ACM on Asia Conference on Computer and Communications Security*, 2017, pp. 506–519.
- [17] P.-Y. Chen, H. Zhang, Y. Sharma, J. Yi, and C.-J. Hsieh, "Zoo: Zeroth order optimization based black-box attacks to deep neural networks without training substitute models," in *the 10th ACM workshop on artificial intelligence and security*, 2017, pp. 15–26.
- [18] A. Ilyas, L. Engstrom, and A. Madry, "Prior convictions: Black-box adversarial attacks with bandits and priors," in *International Conference on Learning Representations (ICLR)*, 2019.
- [19] S. Cheng, Y. Dong, T. Pang, H. Su, and J. Zhu, "Improving black-box adversarial attacks with a transfer-based prior," in *Advances in Neural Information Processing Systems (NeurIPS)*, 2019, pp. 10934–10944.
- [20] A. Al-Dujaili and U.-M. O'Reilly, "Sign bits are all you need for black-box attacks," in *International Conference on Learning Representations (ICLR)*, 2019.
- [21] C. Guo, J. Gardner, Y. You, A. G. Wilson, and K. Weinberger, "Simple black-box adversarial attacks," in *International Conference on Machine Learning (ICML)*, 2019, pp. 2484–2493.
- [22] M. Andriushchenko, F. Croce, N. Flammarion, and M. Hein, "Square attack: A query-efficient black-box adversarial attack via random search," in *the European Conference on Computer Vision (ECCV)*, 2020, pp. 484–501.
- [23] Y. Dong, F. Liao, T. Pang, H. Su, J. Zhu, X. Hu, and J. Li, "Boosting adversarial attacks with momentum," in *the IEEE/CVF Conference on Computer Vision and Pattern Recognition (CVPR)*, 2018, pp. 9185–9193.
- [24] C. Xie, Z. Zhang, Y. Zhou, S. Bai, J. Wang, Z. Ren, and A. L. Yuille, "Improving transferability of adversarial examples with input diversity," in *the IEEE/CVF Conference on Computer Vision and Pattern Recognition (CVPR)*, 2019, pp. 2730–2739.
- [25] Y. Guo, Z. Yan, and C. Zhang, "Subspace attack: Exploiting promising subspaces for query-efficient black-box attacks," in *Advances in Neural Information Processing Systems (NeurIPS)*, 2019, pp. 3820–3829.
- [26] J. Du, H. Zhang, J. T. Zhou, Y. Yang, and J. Feng, "Query-efficient meta attack to deep neural networks," in *International Conference on Learning Representations (ICLR)*, 2019.
- [27] J. Yang, Y. Jiang, X. Huang, B. Ni, and C. Zhao, "Learning black-box attackers with transferable priors and query feedback," in *Advances in Neural Information Processing Systems (NeurIPS)*, vol. 33, 2020.
- [28] S. Chen, Z. He, C. Sun, and X. Huang, "Universal adversarial attack on attention and the resulting dataset DAmageNet," in *IEEE Transactions on Pattern Analysis and Machine Intelligence (TPAMI)*, 2021, pp. 1–1.
- [29] S. Chen, F. He, X. Huang, and K. Zhang, "Relevance attack on detectors," in *Pattern Recognition (PR)*, 2022, p. 108491.
- [30] C. Ma, L. Chen, and J. Yong, "Simulating unknown target models for query-efficient black-box attacks," in *the IEEE/CVF Conference on Computer Vision and Pattern Recognition (CVPR)*, 2021.
- [31] M. Zhou, J. Wu, Y. Liu, S. Liu, and C. Zhu, "Dast: Data-free substitute training for adversarial attacks," in *the IEEE/CVF Conference on Computer Vision and Pattern Recognition (CVPR)*, 2020, pp. 234–243.
- [32] J. Deng, W. Dong, R. Socher, L.-J. Li, K. Li, and L. Fei-Fei, "Imagenet: A large-scale hierarchical image database," in *the IEEE/CVF Conference on Computer Vision and Pattern Recognition (CVPR)*, 2009, pp. 248–255.
- [33] Baidu, "EasyDL: A zero-threshold AI development platform," <https://ai.baidu.com/easydl>, 2019.
- [34] S. Zagoruyko and N. Komodakis, "Wide residual networks," in *British Machine Vision Conference (BMVC)*, R. C. Wilson, E. R. Hancock, and W. A. P. Smith, Eds., 2016.
- [35] Y. LeCun, C. Cortes, and C. Burges, "Mnist handwritten digit database," *ATT Labs [Online]*. Available: <http://yann.lecun.com/exdb/mnist>, vol. 2, 2010.
- [36] A. Krizhevsky *et al.*, "Learning multiple layers of features from tiny images," 2009.
- [37] M. Tan, B. Chen, R. Pang, V. Vasudevan, M. Sandler, A. Howard, and Q. V. Le, "Mnasnet: Platform-aware neural architecture search for mobile," in *the IEEE/CVF Conference on Computer Vision and Pattern Recognition (CVPR)*, 2019, pp. 2820–2828.
- [38] C. Szegedy, W. Zaremba, I. Sutskever, J. Bruna, D. Erhan, I. J. Goodfellow, and R. Fergus, "Intriguing properties of neural networks," in *International Conference on Learning Representations (ICLR)*, 2014.
- [39] Y. Dong, T. Pang, H. Su, and J. Zhu, "Evading defenses to transferable adversarial examples by translation-invariant attacks," in *the IEEE/CVF Conference on Computer Vision and Pattern Recognition (CVPR)*, 2019, pp. 4312–4321.
- [40] Y. Guo, Q. Li, and H. Chen, "Backpropagating linearly improves transferability of adversarial examples," in *Advances in Neural Information Processing Systems (NeurIPS)*, 2020.
- [41] W. Brendel, J. Rauber, and M. Bethge, "Decision-based adversarial attacks: Reliable attacks against black-box machine learning models," in *International Conference on Learning Representations (ICLR)*, 2018.
- [42] J. Chen, M. I. Jordan, and M. J. Wainwright, "HopSkipJumpAttack: A query-efficient decision-based attack," in *the IEEE Symposium on Security and Privacy (SP)*, 2020, pp. 1277–1294.
- [43] M. Cheng, S. Singh, P. H. Chen, P.-Y. Chen, S. Liu, and C.-J. Hsieh, "Sign-opt: A query-efficient hard-label adversarial attack," in *International Conference on Learning Representations (ICLR)*, 2019.
- [44] A. N. Bhagoji, W. He, B. Li, and D. Song, "Practical black-box attacks on deep neural networks using efficient query mechanisms," in *the European Conference on Computer Vision (ECCV)*, 2018, pp. 154–169.
- [45] J. Li, R. Ji, H. Liu, J. Liu, B. Zhong, C. Deng, and Q. Tian, "Projection & probability-driven black-box attack," in *the IEEE/CVF Conference on Computer Vision and Pattern Recognition (CVPR)*, 2020, pp. 362–371.
- [46] C. Ma, S. Cheng, L. Chen, and J. Yong, "Switching gradient directions for query-efficient black-box adversarial attacks," *arXiv preprint arXiv:2009.07191*, 2020.
- [47] Y. Feng, B. Wu, Y. Fan, L. Liu, Z. Li, and S. Xia, "Boosting black-box attack with partially transferred conditional adversarial distribution," *arXiv preprint arXiv:2006.08538*, 2020.

- [48] B. Zoph and Q. V. Le, “Neural architecture search with reinforcement learning,” in *International Conference on Learning Representations (ICLR)*, 2017.
- [49] B. Zoph, V. Vasudevan, J. Shlens, and Q. V. Le, “Learning transferable architectures for scalable image recognition,” in *the IEEE/CVF Conference on Computer Vision and Pattern Recognition (CVPR)*, 2018, pp. 8697–8710.
- [50] E. Real, A. Aggarwal, Y. Huang, and Q. V. Le, “Regularized evolution for image classifier architecture search,” in *the AAAI conference on Artificial Intelligence (AAAI)*, vol. 33, 2019, pp. 4780–4789.
- [51] H. Liu, K. Simonyan, and Y. Yang, “Darts: Differentiable architecture search,” in *International Conference on Learning Representations (ICLR)*, 2019.
- [52] Y. Xu, L. Xie, X. Zhang, X. Chen, G.-J. Qi, Q. Tian, and H. Xiong, “Pc-darts: Partial channel connections for memory-efficient architecture search,” in *International Conference on Learning Representations (ICLR)*, 2020.
- [53] U. Ozbulak, E. T. Anzaku, W. De Neve, and A. Van Messem, “Selection of source images heavily influences the effectiveness of adversarial attacks,” *arXiv preprint arXiv:2106.07141*, 2021.
- [54] G. Hinton, O. Vinyals, and J. Dean, “Distilling the knowledge in a neural network,” *arXiv preprint arXiv:1503.02531*, 2015.
- [55] F. Tramèr, F. Zhang, A. Juels, M. K. Reiter, and T. Ristenpart, “Stealing machine learning models via prediction apis,” in *the USENIX Security Symposium*, 2016, pp. 601–618.
- [56] T. Orekondy, B. Schiele, and M. Fritz, “Knockoff nets: Stealing functionality of black-box models,” in *the IEEE/CVF Conference on Computer Vision and Pattern Recognition (CVPR)*, 2019, pp. 4954–4963.
- [57] A. Ilyas, L. Engstrom, A. Athalye, and J. Lin, “Black-box adversarial attacks with limited queries and information,” in *International Conference on Machine Learning (ICML)*, 2018, pp. 2142–2151.
- [58] Y. Nesterov and V. Spokoiny, “Random gradient-free minimization of convex functions,” *Foundations of Computational Mathematics*, vol. 17, no. 2, pp. 527–566, 2017.
- [59] Y. Zhang, Y. Li, T. Liu, and X. Tian, “Dual-path distillation: A unified framework to improve black-box attacks,” in *International Conference on Machine Learning (ICML)*, 2020, pp. 11 163–11 172.
- [60] G. Huang, Z. Liu, L. van der Maaten, and K. Q. Weinberger, “Densely connected convolutional networks,” in *the IEEE/CVF Conference on Computer Vision and Pattern Recognition (CVPR)*, 2017, pp. 2261–2269.
- [61] K. He, X. Zhang, S. Ren, and J. Sun, “Identity mappings in deep residual networks,” in *the European Conference on Computer Vision (ECCV)*, 2016, pp. 630–645.
- [62] X. Dong and Y. Yang, “Searching for a robust neural architecture in four gpu hours,” in *the IEEE/CVF Conference on Computer Vision and Pattern Recognition (CVPR)*, 2019, pp. 1761–1770.
- [63] D. Han, J. Kim, and J. Kim, “Deep pyramidal residual networks,” in *the IEEE/CVF Conference on Computer Vision and Pattern Recognition (CVPR)*, 2017, pp. 5927–5935.
- [64] C. Szegedy, V. Vanhoucke, S. Ioffe, J. Shlens, and Z. Wojna, “Rethinking the inception architecture for computer vision,” in *the IEEE/CVF Conference on Computer Vision and Pattern Recognition (CVPR)*, 2016, pp. 2818–2826.
- [65] S. Xie, R. Girshick, P. Dollár, Z. Tu, and K. He, “Aggregated residual transformations for deep neural networks,” in *the IEEE/CVF Conference on Computer Vision and Pattern Recognition (CVPR)*, 2017, pp. 1492–1500.
- [66] A. Paszke, S. Gross, F. Massa, A. Lerer, J. Bradbury, G. Chanan, T. Killeen, Z. Lin, N. Gimelshein, L. Antiga *et al.*, “Pytorch: An imperative style, high-performance deep learning library,” in *Advances in Neural Information Processing Systems (NeurIPS)*, 2019, pp. 8024–8035.
- [67] hysts, “Github repository for image classification by pytorch,” https://github.com/hysts/pytorch_image_classification.
- [68] S. N. Shukla, A. K. Sahu, D. Willmott, and J. Z. Kolter, “Black-box adversarial attacks with bayesian optimization,” *arXiv preprint arXiv:1909.13857*, 2019.
- [69] K. He, X. Zhang, S. Ren, and J. Sun, “Deep residual learning for image recognition,” in *the IEEE/CVF Conference on Computer Vision and Pattern Recognition (CVPR)*, 2016, pp. 770–778.
- [70] H. Li, S. Shan, E. Wenger, J. Zhang, H. Zheng, and B. Y. Zhao, “Blacklight: Defending black-box adversarial attacks on deep neural networks,” *arXiv preprint arXiv:2006.14042*, 2020.
- [71] Z. Qin, Y. Fan, H. Zha, and B. Wu, “Random noise defense against query-based black-box attacks,” in *Advances in Neural Information Processing Systems (NeurIPS)*, 2021, pp. 7650–7663.
- [72] S. Chen, Z. Huang, Q. Tao, Y. Wu, C. Xie, and X. Huang, “Adversarial attack on attackers: Post-process to mitigate black-box score-based query attacks,” in *Advances in Neural Information Processing Systems (NeurIPS)*, 2022.
- [73] Y. Wu, S. Chen, K. Fang, and X. Huang, “Unifying gradients to improve real-world robustness for deep networks,” *arXiv preprint arXiv:2208.06228*, 2022.
- [74] A. Athalye, N. Carlini, and D. Wagner, “Obfuscated gradients give a false sense of security: Circumventing defenses to adversarial examples,” in *International Conference on Machine Learning (ICML)*, 2018, pp. 274–283.
- [75] D. Su, H. Zhang, H. Chen, J. Yi, P.-Y. Chen, and Y. Gao, “Is robustness the cost of accuracy?—a comprehensive study on the robustness of 18 deep image classification models,” in *the European Conference on Computer Vision (ECCV)*, 2018.
- [76] S. Chen, Q. Tao, Z. Ye, and X. Huang, “Going far boosts attack transferability, but do not do it,” *arXiv preprint arXiv:2102.10343*, 2021.
- [77] C. Malherbe and N. Vayatis, “Global optimization of lipschitz functions,” in *International Conference on Machine Learning (ICML)*, 2017, pp. 2314–2323.
- [78] Y. Cai, C. Wang, X. Ning, Z. Zhou, D. Niu, H. Yang, and Y. Wang, “Deepguiser: Learning to disguise neural architectures for impeding adversarial transfer attacks,” 2023.



Sizhe Chen received his B.E. and M.E. degree in Shanghai Jiao Tong University, Shanghai, China, in 2020 and 2023, respectively. He is a Ph.D. student at the Department of Electrical Engineering and Computer Sciences, University of California, Berkeley. His research interests are focused on trustworthy machine learning.



Zhehao Huang received his B.E. degree in Shanghai Jiao Tong University, Shanghai, China, in 2022. He is now a Ph.D. student at the Institute of Image Processing and Pattern Recognition, Shanghai Jiao Tong University, Shanghai, China. His research interests are architecture design and sparsity of DNNs.



Qinghua Tao received the B.S. degree from Central South University, China, in 2014, and the Ph.D. degree from Tsinghua University, China, in 2020. She is currently a Post-Doctoral Researcher with ESAT-STADIUS, KU Leuven, Belgium. Her research interests include machine learning, dynamic systems and optimization, especially for the analysis and applications of piecewise linear neural networks.



Xiaolin Huang (S'10-M'12-SM'18) received the B.S. degree in control science and engineering, and the B.S. degree in applied mathematics from Xi'an Jiaotong University, Xi'an, China in 2006. In 2012, he received the Ph.D. degree in control science and engineering from Tsinghua University, Beijing, China. From 2012 to 2015, he worked as a postdoctoral researcher in ESAT-STADIUS, KU Leuven, Leuven, Belgium. After that he was selected as an Alexander von Humboldt Fellow and working in Pattern Recognition Lab, the Friedrich-Alexander-Universität Erlangen-Nürnberg, Erlangen, Germany. From 2016, he has been an Associate Professor at Institute of Image Processing and Pattern Recognition, Shanghai Jiao Tong University, Shanghai, China. In 2017, he was awarded by "1000-Talent Plan" (Young Program).

His current research areas include machine learning and optimization, especially for robustness and sparsity of both kernel learning and deep neural networks.

APPENDIX

A. Attackers in QueryNet

In the forward propagation of QueryNet, one could flexibly choose diverse attackers. Here we specify a feasible and efficient design of attackers, which contain model-dependent and model-independent attacks.

Model-dependent attacks are to attack surrogates and generate AEs based on the attack transferability. Here we want a fast attack to accelerate the fooling, and thus choose FGSM [6], which is also preferred due to its good transferability [75]. Multi-step attacks, like Projected Gradient Descend [9] and its transferability enhance techniques [23], [39], have been tested in QueryNet but are not as efficient as FGSM. With FGSM, line 1 in Alg. 1 is specified as

$$X_i = \begin{cases} \text{clip}_{X^{\text{org}}}^\varepsilon(X + 2\varepsilon \cdot \text{sign}(\nabla_{\mathbf{x}} \mathcal{L}(\mathcal{S}_i(X), Y))), & p = \infty, \\ \text{rescale}_{X^{\text{org}}}^\varepsilon(X + 2\varepsilon \cdot \frac{\nabla_{\mathbf{x}} \mathcal{L}(\mathcal{S}_i(X), Y)}{\|\nabla_{\mathbf{x}} \mathcal{L}(\mathcal{S}_i(X), Y)\|_2}), & p = 2, \end{cases}$$

where $\text{clip}(\cdot)$ denotes that the pixels being directly clipped into the bound ε as in [9], and $\text{rescale}(\cdot)$ means the perturbation $X' - X$ is rescaled to the ℓ_2 bound as in [22], [27]. We modify the step size to 2ε to ensure that every pixel reaches the bound at all iterations, enhancing the transferability [76].

Model-independent attacks, mainly referring to random-search attacks [21], [22], [45], do not rely on surrogates. In our study, we select the excellent SOTA Square attack [22], which adds a random-generated square to the current perturbation in each iteration. Square attack initializes the perturbation by random vertical stripes to boost the fooling, which is also adopted in QueryNet.

In this random-search attack, past query pairs from the same original sample are not taken into account for reducing queries. To take full use of this information, we resort to the sequential search approach for black-box optimization problems, where the goal, similar to the iterative query, is to find the optimum with a small budget of function evaluation times. To achieve that, [77] develops a mechanism to evaluate only the promising samplings, termed potential maximizers. Inspired by that, we propose Square+ to yield a candidate AE only if it is the potential maximizer. Otherwise, we retry the random search on the square location until it reaches a maximum times M . A sample x^q (labeled y) is a potential maximizer, according to [77], if and only if it satisfies the Lipschitz continuity assumption on the victim's loss, i.e.,

$$\max_{i \neq j} \frac{|\mathcal{L}(\mathcal{V}(\mathbf{q}_i), y) - \mathcal{L}(\mathcal{V}(\mathbf{q}_j), y)|}{\|\mathbf{q}_i - \mathbf{q}_j\|_2} \|\mathbf{x}^q - \mathbf{q}_i\|_2 - \max_i \mathcal{L}(\mathcal{V}(\mathbf{q}_i), y) \geq -\beta \min_i \mathcal{L}(\mathcal{V}(\mathbf{q}_i), y), \quad (5)$$

where \mathbf{q}_i is the i^{th} queried AE for the original sample of \mathbf{x}^q , and β is the hyper-parameter to decide the tightness of this constraint. In our implementation, we heuristically choose $\beta = 0.7$ and $M = 50$. The first term in (5) involves the estimated Lipschitz constant from all past query samples. Aware on that, Square+ improves the attack diversity and boosts the query-efficiency further, seeing our ablation study.

B. The attacker evaluation weights

In the backward propagation of QueryNet, the surrogates' weights for ensemble and evaluation w can also be calibrated by the query information. The weight reflects the quality of a surrogate. Accordingly, we set it as the ratio of its yielded AEs that become more adversarial to V as

$$w_i = \frac{\#\mathbf{a}_I(i)}{\#\mathbf{a}(i)}, \quad I = \{k : \mathcal{L}(\mathcal{V}(X_k^q), Y_k^{\text{org}}) < L_k\}, \quad (6)$$

where \mathbf{a} is the selected attacker index in the forward propagation (3), and $\#\mathbf{a}(i)$ denotes the times that i appears in \mathbf{a} , i.e., the number of X^q that come from candidate AEs X_i crafted by A_i . $\#\mathbf{a}_I(i)$ refers to the number of X^q from X_i that become more adversarial to the victim, because the set I contains the indexes of the query samples that decrease the victim's loss L . Generally, if AEs from one attacker are frequently selected, its evaluation weight would be large. In an extreme case, $w_i = 0$ if $\#\mathbf{a}(i) = 0$, i.e., no candidate AE from S_i is selected, so its quality is low. The evaluation weight for a surrogate signifies its quality compared to others. Thus, in the beginning, all n surrogates are considered equally important with the same weight, namely $[w_1, w_2, \dots, w_n] = \mathbf{1}$.

By calibrating surrogates' quality, QueryNet's AE evaluation mechanism (3) becomes more accurate. Besides evaluation, it is interesting to notice that (6) is also applicable to measure the quality of model-independent attackers. Based on this, we design a strategy to balance different attackers for good query-efficiency and time-efficiency. We initialize the attacker weight for Square+ (attacker $n+1$) and Square (attacker $n+2$) as zero. In the beginning, the prior knowledge is important, so we adopt surrogate attackers and Square+ since they are based on past query information. After the surrogate attackers' quality becomes lower than random-search attacks, we resort to Square+ and Square. Finally, the estimated Lipschitz in Square+ would be also inaccurate [77], and we use only Square, where it would be unnecessary to evaluate candidate AEs generated from one method, so the computational costly training of surrogates is terminated. This strategy could be expressed as $\{\mathcal{A}_i\} =$

$$\begin{cases} \mathcal{A}_1 \rightarrow \mathcal{A}_{n+1}, & w_{n+1} < \max(w_1 \rightarrow w_n), \\ \mathcal{A}_{n+1}, \mathcal{A}_{n+2}, & \max(w_1 \rightarrow w_n) < w_{n+1}, w_{n+1} < w_{n+2}, \\ \mathcal{A}_{n+2}, & w_{n+2} > \max(w_1 \rightarrow w_{n+1}). \end{cases}$$

We illustrate the process above by an example in Fig. 5. QueryNet adaptively selects the most efficient attacker for every AE, so different methods work on a dynamic proportion of samples. Although this strategy is heuristically designed, it generalizes to different settings without careful modification.

C. Hyper-parameters for baselines

For a fair and unbiased comparison, we inherit most hyper-parameters but carefully tune crucial ones in all compared methods for good performance.

Bandits is a gradient estimation query attack, so we mainly tune the finite-difference step size. Considering its low query-efficiency, we only evaluate the step size 0.1 (original) and 1.0 for CIFAR10 in our 8-bit query setting. The attack success rate is higher at 0.1, while the A.Q. is lower at 1.0. For a trade-off,

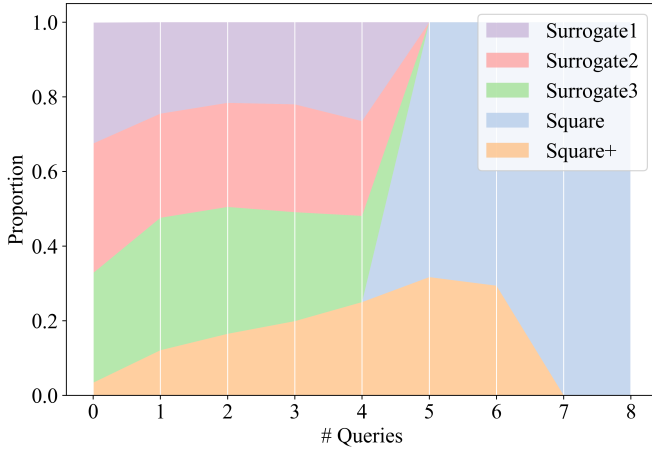


Fig. 5: Proportion of functional attackers. In iteration $0 \rightarrow 4$, we adopt surrogate attackers and Square+. As surrogates’ transferability effect decreases, QueryNet automatically switches to Square+ and Square in iteration $4 \rightarrow 7$. Finally, the Square takes the lead, generating the most effective AEs, and are thus used solely after iteration 7. The results are produced by WRN28 on CIFAR10 with $\ell_2 = 3$.

we set the finite-difference step size 0.1 on both CIFAR10 and MNIST for ℓ_2 and ℓ_∞ attacks.

SimBA is a random-search attack. For MNIST, its attack step size 1.0 makes a significant improvement of high attack success rate and low average query times compared with the original step size 0.1, so we choose 1.0 in all evaluations.

LeBA is based on SimBA with additional surrogate models. We set the step size following SimBA and pay more attention to the choice of surrogate models. We comprehensively evaluate ResNet152, DenseNet121, and DenseNet201 for CIFAR10 and select the best-performed ResNet152.

PPBA is a random-search attack. We mainly tune the dimension of the measurement vectors and the change of vector amplitude value ρ . We set the dimension as 1500 for ImageNet following the original settings and also for CIFAR10, but we reduce the dimension to 350 for MNIST. We also try to explore the most effective ρ in our 8-bit query setting by evaluating $\rho = 0.01, 0.03, 0.05$ for ℓ_2 attacks and $\rho = 0.01, 0.03, 0.1, 0.3, 1.0, 3.0$ for ℓ_∞ attacks. Based on the results, we set the best $\rho = 0.01$ for ℓ_2 attacks and $\rho = 1.0$ for ℓ_∞ attacks in MNIST, CIFAR10, and ImageNet.

Subspace is a gradient estimation query attack with surrogates. We use all pre-trained surrogates in the official implementation, i.e., AlexNet and VGGNets for CIFAR10 and ResNet-18/34/50 for ImageNet. We also evaluate the finite-difference step size of 0.1 (original), 1.0, and 2.0 for CIFAR10 and 0.1, 0.5, 1.0, 3.0 for ImageNet. We finally set step size as 1.0 for CIFAR10 and step size as 3.0 and 1.0 for ImageNet on ℓ_2 and ℓ_∞ attacks respectively.

Square is a random-search attack. We inherit the official strategy to gradually decrease the size of squares but set the probability of changing a coordinate $p = 0.05$ for all attacks, which is validated better against the original $p = 0.1$ in ℓ_2 attacks.

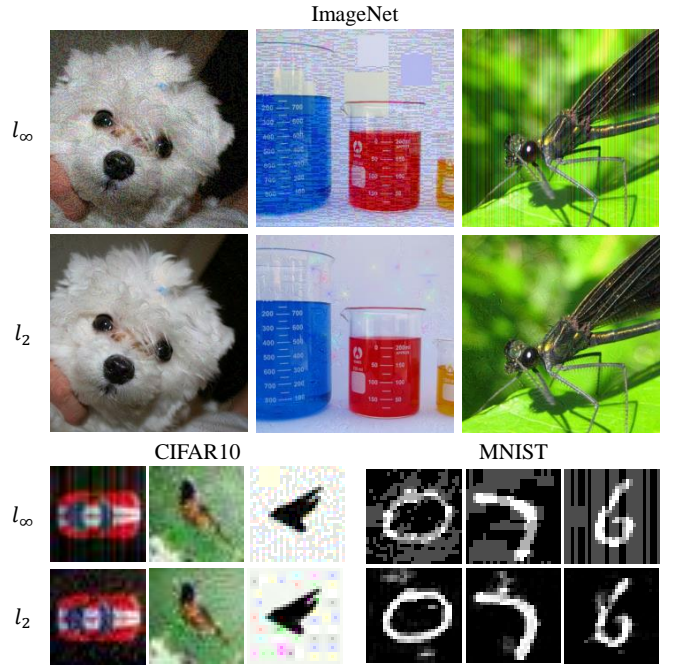


Fig. 6: QueryNet AEs. AEs are from attacks on MNASN (ImageNet), EasyDL (CIFAR10), and DN40 (MNIST).

D. QueryNet adversarial examples

We visualize the adversarial examples generated by QueryNet in Fig. 6, where it is interesting to see the balanced effect of Square attack and FGSM, i.e., the perturbations are constructed by squares and adversarial noise. It illustrates that QueryNet improves the query-efficiency by a dynamic and learnable balance between random-search attack and transfer attack.

E. QueryNet searched architectures

We visualize surrogates’ architectures searched by QueryNet in Fig. 7, where we could see that surrogates (with different No. layers) would end with different cells stealing the victim despite training in the same data and searching in the same architecture space.

QueryNet’s success lies in the simultaneous achievement of prediction similarity and gradient similarity via additionally altering the surrogate’s architecture. This greater optimization space improves the approximation to the victim, so the query efficiency is significantly boosted despite that we cannot steal the exact architecture merely through observing outputs [78].

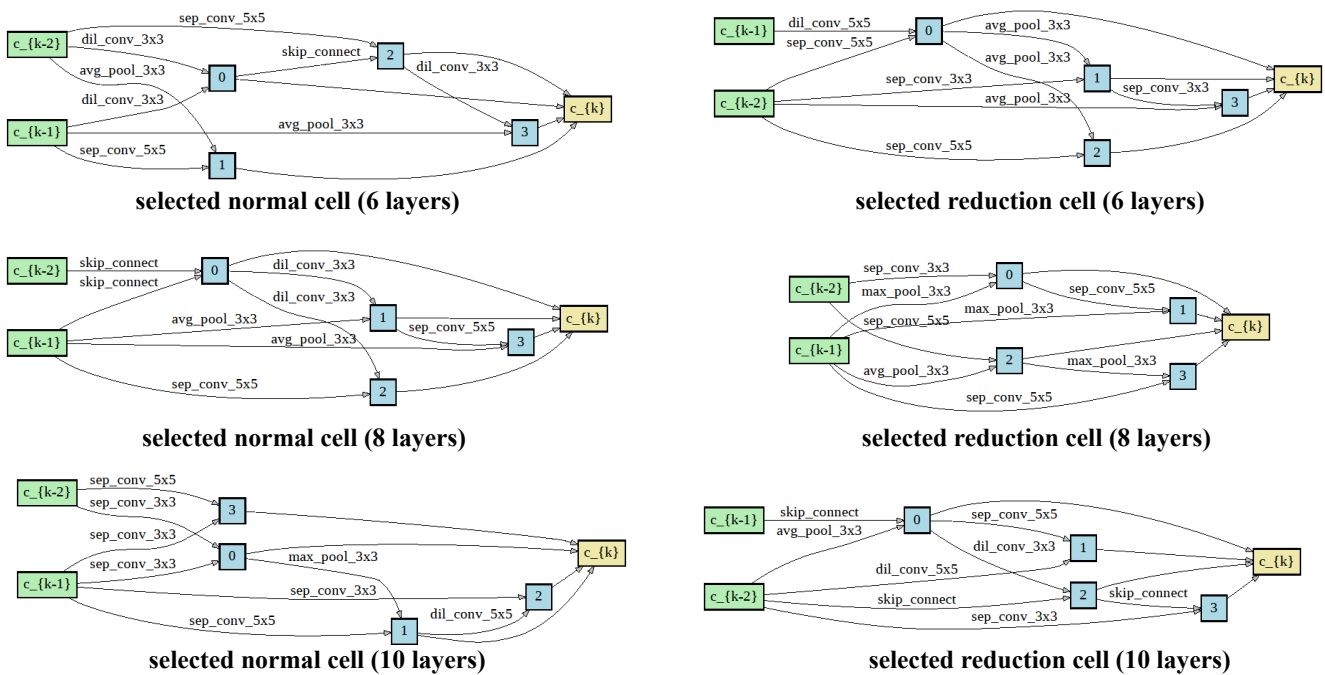


Fig. 7: The searched surrogate’s architecture by QueryNet when attacking a CIFAR-10 WideResNet28 model to craft 10K samples. All surrogates are trained for 7 attack iterations using randomly sampled data from past query pairs.